BUTTERWORTH HEINEMANN

Polymer Vol. 36 No. 15, pp. 2867–2872, 1995

0032-3861/95/$10.00 + 0.00

polymer papers

Electrically conductive polymer fibres with mesoscopic diameters: 1. Studies of structure and electrical properties

M. Granström* and O. Inganäs
Laboratory of Applied Physics, Department of Physics (IFM), University of Linköping, S-581 83 Linköping, Sweden
(Received 15 August 1994; revised 6 February 1995)

Different types of conductive polymers have been synthesized within the pores of nanoporous microfiltration membranes. These membranes contain linear, cylindrical pores of varying diameter from 10 nm to 10 μm. When synthesized within these pores, the conductivity of the polymer increases compared to the conductivity of a polymer film synthesized on a planar electrode. The enhancement in conductivity increases with decreasing pore diameter. In addition to the electrical measurements, X-ray diffraction, computer modelling and infra-red spectroscopy have been used to evaluate the structural properties of these polymer fibres. The level of enhancement is also shown to be dependent on the type of monomer and counterion used in the polymerization.

(Keywords: conductive polymers; structure; conductivity)

INTRODUCTION

A number of aromatic molecules have been shown to polymerize electrochemically. Among these we find conductive polymers with properties that are applicable in areas like electronic devices[1], optronics[2], advanced batteries[3] and environmental sensors[4]. In this group of polymers we find poly(pyrrole) and poly(thiophene) and their derivatives. In this study some of these polymers were synthesized electrochemically in a specific geometry: within narrow, cylindrical pores. These pores can be found in commercially available microfiltration membranes, and this method has been developed by Martin and coworkers[5,6] and Calahane and Labes[7]. This method has also been extended to metals and electrochemically preparable II–VI semiconductors[8]. The membranes are made of poly(carbonate) or poly(ester) and the pores are fabricated using a nuclear track-etching process, giving randomly distributed holes with well-defined diameters between 10 nm and 14 μm. It has been shown that this geometrically restricted polymerization can change some of the properties of the conductive polymer, such as increasing the conductivity dramatically[9] and giving unique morphologies[7]. The resulting composite polymer membranes are in this study characterized by the transverse resistivity and calculation of the conductivity of the individual conducting fibres. To study the structure of the polymers, X-ray diffraction combined with computer simulations and i.r. spectroscopy were used.

* To whom correspondence should be addressed

EXPERIMENTAL

Host membranes

Nuclepore® and Poretics® poly(carbonate) microfiltration membranes were used. In our experiments we used pore sizes of 10 nm, 100 nm, 1 μm and 10 μm to accomplish a wide range of geometrical constraints. The thickness of the membrane varied between 6 and 11 μm and the number of pores ranged from 10^5 to 6×10^8 pores cm^{-2}. The membranes were attached to gold contacts on glass substrates as reported earlier[10].

Polymerization

Different conjugated polymers were studied: poly(pyrrole) (PPy) with different counterions, poly(*N*-methylpyrrole) (PMPy), poly(dithiopheneoctylthiophene) (PDTOT)[11] and poly(3,4-ethylenedioxythiophene) (PEDOT)[12]. Their chemical structures are shown in *Figure 1*. All monomers were polymerized electrochemically using a Bioanalytical Systems BAS100A electrochemical analyser and a three-electrode cell with a platinum foil as the counterelectrode and Ag/AgCl as the reference electrode.

Poly(pyrrole) was synthesized in three different ways from 0.1 M pyrrole together with (1) 0.5 M $LiClO_4$ in distilled water (PPy/ClO); (2) 0.5 M tetraethylammonium toluenesulfonate in distilled water (PPy/TS); or (3) a polymeric ion (proprietary material, CIBA-GEIGY), roughly 0.5 M, in propylene carbonate (PPy/Pol). Potentials between 0.8 and 1.1 V vs. Ag/AgCl were used.

Poly(*N*-methylpyrrole) was made from 0.1 M *N*-methylpyrrole and 0.5 M $LiClO_4$ in acetonitrile. The potential used was 800 mV vs. Ag/AgCl.

Poly(dithiopheneoctylthiophene) was made from 0.1 M thiopheneoctylthiophenethiophene monomer and

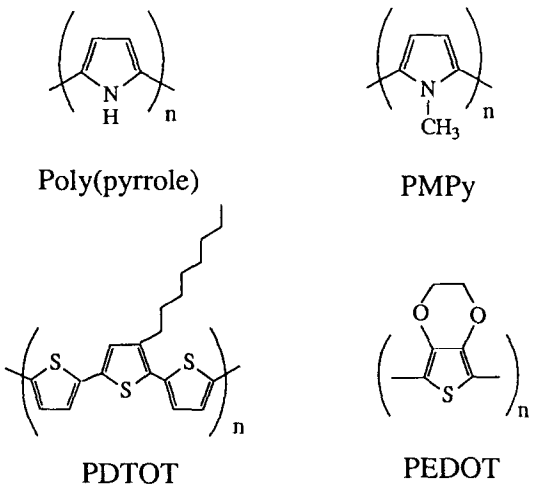

Figure 1 Chemical structures of the polymers

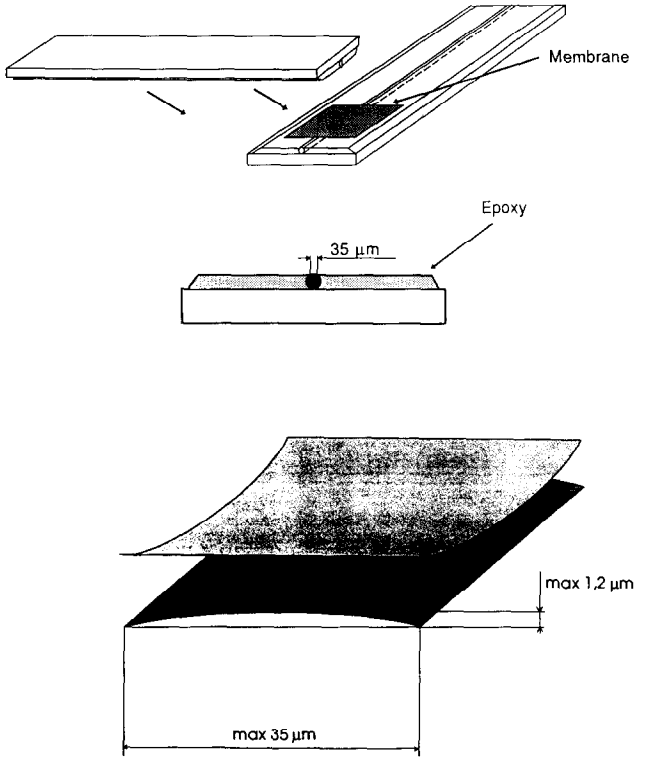

Figure 2 Conductivity measurement geometry

0.5 M $LiClO_4$ in acetonitrile. A suitable polymerization voltage was chosen by cyclic voltammetry as 800 mV vs. Ag/AgCl.

Poly(3,4-ethylenedioxythiophene) was made from 0.5 M monomer and 0.5 M $LiClO_4$ in acetonitrile. For this polymerization a potential of 1.3 V vs. Ag/AgCl was needed.

Conductivity measurements

The conductivity of the polymer in the pores was measured using a technique with thin Au wires (diameter 0.25 mm) embedded in epoxy (see *Figure 2*), one on each side of the membrane. Although this is a two-point technique, it gives a sufficiently well-defined cross-section for measuring the conductivity consisting of a cylindrical surface that has a maximum 'penetration' into the

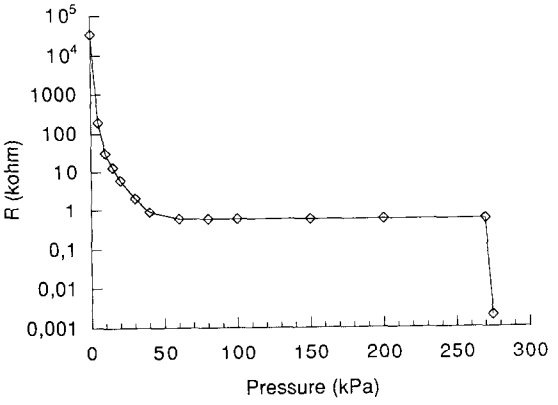

Figure 3 Resistance through the membrane as a function of applied pressure

Table 1 X-ray parameters

Parameter	Details
Radiation	CuKα, Ni filtered
Power	40 kV, 20 mA
2θ range	2–28°
Step width	0.02°
Count time	10 s per step
Temperature	20°C

membrane of 1.2 μm, as can be seen in *Figure 2*. It has also been shown that four-point probe measurements corroborate the two-point results[13]. The numbers established in this way will give a lower limit for the conductivity of the single fibres, since it is assumed in the calculations that all tubes will be fully grown throughout the membrane. Since the pores are initiated using a point-shaped radiation source, all of them will not be oriented perfectly perpendicular to the membrane surface, but with angles deviating slightly from 90°. This means that some pores are somewhat longer than others, and there will be small differences in how far the conducting polymer has grown. There could also be differences between the polymer fibres grown at the centre of the membrane and close to the edge. As shown in *Figure 3*, there is a pressure dependence when measuring the conductivity. The first part of the curve in *Figure 3* is assumed to have its origin in geometrical factors, since the membranes are somewhat flexible. Very few tubes will then be contacted if the gold wires are put on each side of the membrane and no pressure applied. When the pressure is increased, more and more tubes will be contacted and the resistance will drop to a stable value. This plateau value is the one used for the conductivity calculations. When the pressure is further increased, the membrane will eventually break and a short circuit is created. This can be seen in the last part of the curve in *Figure 3*. That this model is reasonable is supported by the fact that the pressures in these experiments are much lower than needed to change the density of localized states and thereby the conductivity of the conductive polymer[14].

X-ray diffraction

X-ray data were recorded using a computer-controlled Philips PW1710 diffractometer. In general the parameters in *Table 1* were used. The X-ray data were also

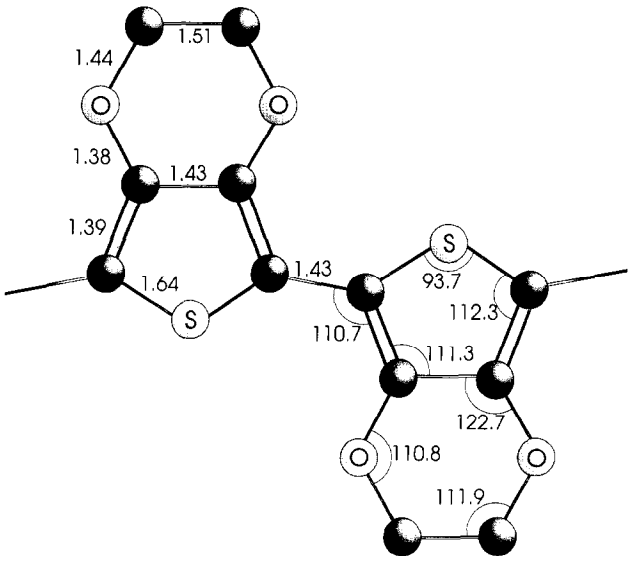

Figure 4 Optimized geometry (bond lengths in angstroms) for PEDOT (result from MOPAC calculation)

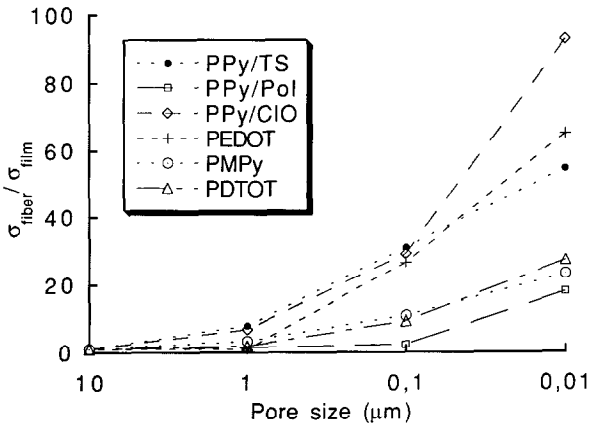

Figure 5 Conductivity of a single polymer fibres as a function of pore size and counterion. The conductivity values are normalized by dividing by the conductivity of a polymer film synthesized on a flat, macroscopic electrode

evaluated using the CERIUS program package from Molecular Simulations Inc. This program makes it possible to build and test different crystal structures for the polymers. For poly(pyrrole) the structures were determined by starting from suitable models found elsewhere[15], inserting the dopant ion and minimizing the energy by changing the position and orientation of the ion, as well as by adjusting the lattice parameters and orientation of the polymer chain along the *c* axis of the lattice. All this was done in an iterative process. Since no calculations on PEDOT have been published, a model was built in CERIUS and optimized using the quantum chemistry program MOPAC[16]. In these calculations the semiempirical AM-1 method[17] was used. The optimized geometry was found to be as in *Figure 4* (not showing the hydrogens), and crystal structures were built starting from polymers of this model and then using the same method as for the pyrrole simulations.

I.r.

Infra-red reflection absorption spectroscopy (i.r.r.a.s.) measurements were made using a Bruker IFS 113v i.r. spectrometer. Samples with empty membranes on a gold surface, PPy/ClO-filled membranes on gold and dissolved membranes leaving the PPy fibres spread out on the gold surface were investigated and the results were compared to spectra from homogeneous films of PPy/ClO.

RESULTS AND DISCUSSION

Electrical conductivity

Figure 5 shows the relationship between pore size and increase in conductivity for the different polymers and polymer/counterion combinations. The presented results are mean values from three to five samples and represent the lower limits of the conductivity in the single fibres as discussed earlier. In *Table 2*, the highest values (10 nm fibres) are listed for each polymer/counterion combination. It is evident that the increase in conductivity is considerable, especially for the smallest pore size (10 nm). It is also clear that there is dependence on the size and type of counterion, since the increase in conductivity is smaller and demands narrower pores for poly(pyrrole) made with the larger, polymeric counterions (PPy/Pol) compared to the samples with smaller ions. This is in agreement with investigations of polymer films made on flat macroelectrodes[18–21]. In these studies it was found that smaller ions are more easily incorporated into the polymer films, but also that certain geometries are favourable. An example of this is that an aromatic counterion such as toluenesulfonate induces anisotropy in poly(pyrrole) films[18] and gives thermally more stable films[20]. As can be seen from *Figure 5*, all the different polymers involved in this investigation show an increase in conductivity of at least 10 times. Taking into account the wide variety of geometries involved in these different polymers and for poly(acetylene)[22], it is unlikely that the increase is only an effect of epitaxy along the pore walls. Rather, it is necessary to investigate the polymerization conditions within the pores compared to a macroscopic flat surface, something that will be addressed in the second part of this series of papers.

Table 2 Conductivity for 10 nm fibres of each polymer/counterion combination and other polymers

Polymer	Conductivity ($S\,cm^{-1}$)
PPy/TS	1.2×10^3
PPy/Pol	180
PPy/ClO	1.3×10^3
PEDOT	780
PMPy	0.045
PDTOT	1.1

In addition to the above-mentioned measurements, the temperature dependence of the conductivity was also investigated for some of the polymers. *Figure 6* shows the results for PPy/ClO and PEDOT, where there is a significant difference in thermal stability above 100°C.

One way of evaluating the results from the temperature dependence measurements is to use the Mott variable range hopping (VRH) theory[23]. This theory is based on a balance between the thermodynamic constraint on a charge carrier moving to a nearby localized state of different energy and the quantum

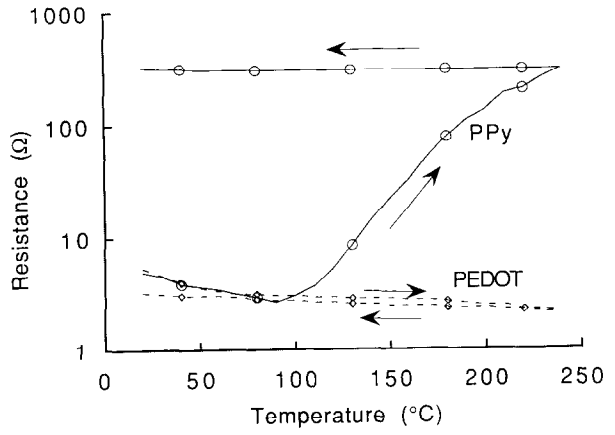

Figure 6 Temperature dependence of the conductivity: comparison between PPy/ClO and PEDOT

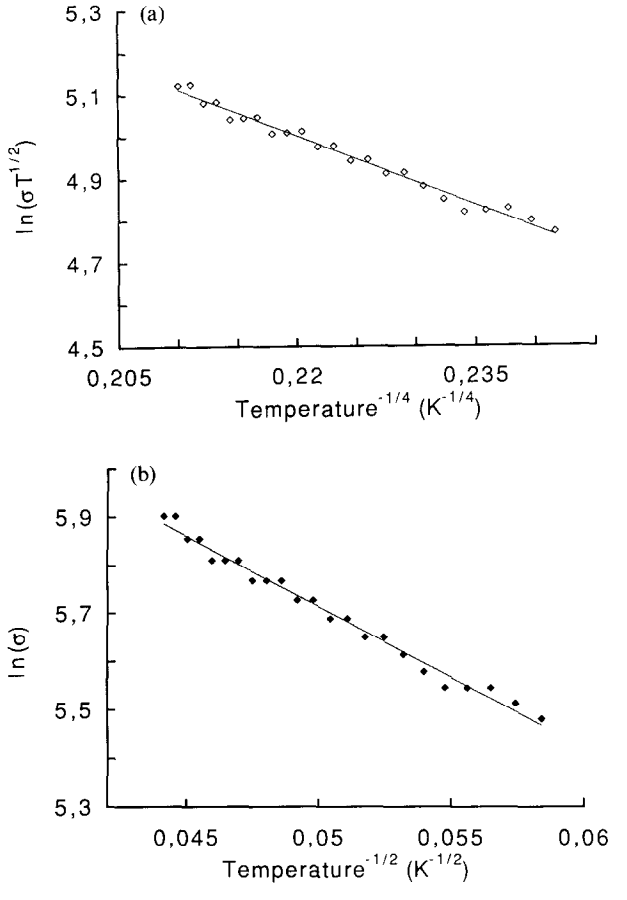

Figure 7 Conductivity–temperature plots for PEDOT: (a) VRH theory; (b) Sheng's theory

mechanical restraint on a carrier moving to a localized state of similar energy but spatially remote. This establishes a temperature dependence of conductivity of the form $\ln\sigma \propto T^{-1/4}$ for three-dimensional hopping. Since there is no restriction regarding the type of charge carrier in the VRH theory, we can apply this to our conductive polymers and the theory predicts the following behaviour

$$\sigma(T) = \frac{\sigma_0}{T^{1/2}} \exp\left[-\left(\frac{T_0}{T}\right)^{1/4}\right] \quad (1)$$

where σ_0 is the conductivity at infinite temperature and T_0 is the characteristic temperature. Plotting $\ln(\sigma T^{1/2})$ vs. $T^{-1/4}$ gives the result shown in *Figure 7a*. Calculating the characteristic values from the fitted line in *Figure 7a* gives $\sigma_0 = 1.6 \times 10^4\ \mathrm{S\,cm^{-1}}$ and $T_0 = 1.47 \times 10^4\ \mathrm{K}$ for PEDOT in our geometry. These values are comparable with typical values for conducting polymers such as poly(pyrrole)[24]. However, this does not exclude the possibility that the conduction through the polymer can occur through highly conducting islands separated by barriers[25,26]. If the islands are less than 20 nm in size, the temperature dependence of the conductivity is[27]

$$\sigma(T) = \sigma_0 \exp\left[-\left(\frac{T_0}{T}\right)^{1/2}\right] \quad (2)$$

The conductivity data for PEDOT evaluated according to this model are shown in *Figure 7b*. Comparing *Figures 7a* and *7b*, it is impossible to decide which mechanism dominates the charge transport in the PEDOT fibres.

X-ray diffraction

For poly(pyrrole) there is normally a very broad and weak diffraction peak centred at about 25° which corresponds to an amorphous material with a mean Bragg spacing of 3.4 Å (1 Å = 0.1 nm)[28]. In our samples we find that when the pore size decreases this peak and a corresponding peak at $2\theta = 12.6°$ (spacing 7.0 Å) increase in intensity and also sharpen considerably (*Figure 8*). For *Figure 8* it should be remembered that the pore density is different for the different samples, where 2.36% of the area consists of pores for the 100 nm samples and 0.092% for the 10 nm samples. The increase and sharpening suggest that the ordering of the material is enhanced when grown in the narrow pores, a result that is in accordance with previous results from Cai *et al.*[9]. There is also a correspondence between the different onsets of the increase in conductivity for different counterions in the conductivity measurements

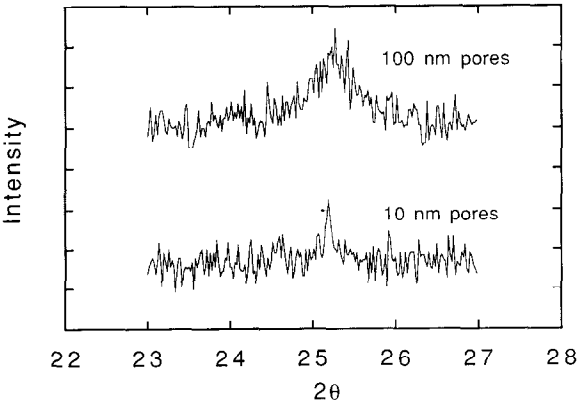

Figure 8 Diffractograms for PPy/TS in 100 and 10 nm pores

Table 3 Calculated lattice structures for poly(pyrrole) doped with two different counterions

Dopant	Doping level (%)	*a* (Å)	*b* (Å)	*c* (Å)	Energy[a] (kcal mol^{-1})
Toluenesulfonate	25	7.00	7.20	14.08	−16.4
Perchlorate	25	7.01	7.13	14.08	−12.8

[a] kcal = 4.2 kJ

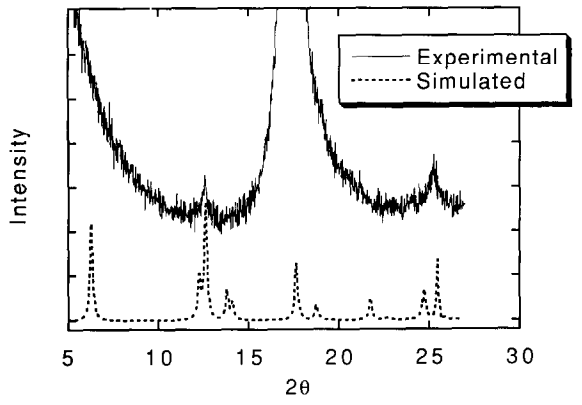

Figure 9 Experimental and simulated diffractograms for PPy/TS in 100 nm pores. The large and broad peak from 16 to 20° in the experimental diffractogram comes from the host membrane (semi-crystalline poly(carbonate))

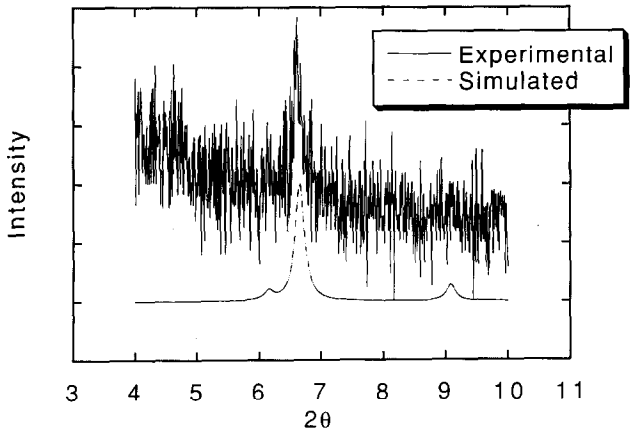

Figure 10 Experimental and simulated diffractograms for PEDOT in 0.1 μm pores

and the intensity and sharpness of the diffraction peaks. For PPy/Pol where the conductivity increase is smaller for the same pore size compared to PPy/ClO and PPy/TS, the diffraction peaks are smaller and sometimes almost impossible to resolve.

Modelling of the poly(pyrrole) structures has given the orthorhombic structures proposed in *Table 3*. *Figure 9* shows a comparison between the calculated (doping level 25%) and measured diffractograms for PPy/TS.

For PEDOT the results are similar, giving a peak at $2\theta = 6.7°$ which suggests a spacing of 13.2 Å. The resulting optimized crystal that gave the closest fit with the experimental results was a 25% doping level (one dopant ion for every four EDOT rings) orthorhombic cell with the cell parameters $a = 13.2$ Å, $b = 4.25$ Å and $c = 14.25$ Å, where the polymer is aligned along the c axis. The dopant ClO_4^- ion is then positioned at $a' = 7.06$ Å, $b' = 2.97$ Å and $c' = 8.60$ Å. In *Figure 10* an experimental diffractogram is shown together with the simulated diffractogram of this structure.

I.r.

Examples of i.r. spectra are shown in *Figure 11*, where the spectrum for PPy fibres is from a sample where the host membrane was dissolved in chloroform and rinsed away after polymerization. The spectrum measured on poly(pyrrole) grown as fibres has sharper and more well-

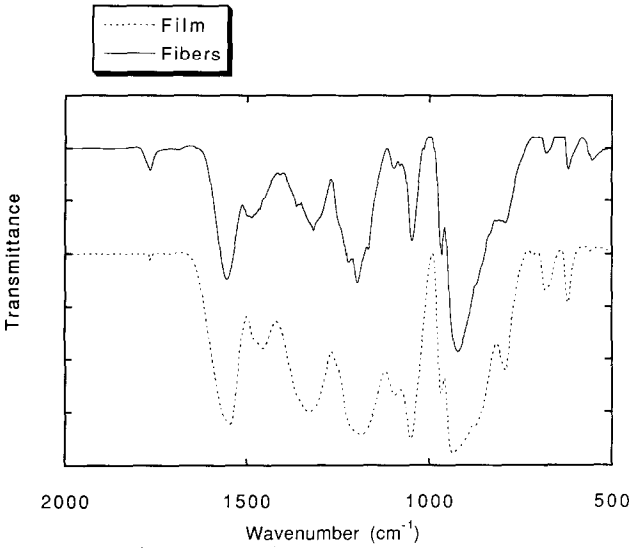

Figure 11 I.r. spectra for homogeneous PPy/ClO film and PPy/ClO fibres

resolved peaks than those found in the reference spectrum measured on a homogeneous poly(pyrrole) film. This indicates ordering of the material and fortifies the results from the X-ray measurements. However, more information can be drawn from the i.r. measurements: Tian and Zerbi[29] have shown that the so-called effective conjugation coordinate (ECC) can be used to calculate the vibrational spectra for poly(pyrrole) and poly(thiophene). The theory predicts that the relative intensities of the absorption bands around 1550 and 1470 cm^{-1} are strongly connected to the delocalization of π-electrons. The ratio between the integrated absorptions at 1550 and 1470 cm^{-1}, $r = I_{1550}/I_{1470}$, then gives a measure of the conjugation length in the polymer (a shorter conjugation length giving larger r). Liang *et al.*[30] have used this to correlate the synthesis temperature and conductivity in PPy films. For PPy/ClO in 100 nm and 10 nm pores the ratios were measured to be $r = 1.9$ and $r = 1.2$, respectively, which should be compared to $r = 4.6$ for the homogeneous film. The value $r = 4.6$ is comparable with the results of Liang *et al.* ($r = 4.9$ for chemically synthesized PPy/ClO at 27°C). The material grown in the pores therefore has a radically longer conjugation length than that found in ordinarily synthesized films, explaining the higher conductivity.

CONCLUSIONS

We have shown that the increase in conductivity and crystallinity of conductive polymers synthesized within narrow pores is behaviour common to a wide variety of heterocyclic polymers. This increase is therefore believed to be an effect not of epitaxy but of the unique polymerization conditions that occur inside the pores. These aspects will be investigated further in part 2 of this series. The crystal structures for some of the polymer/counterion combinations have been modelled and compared to the X-ray measurements. It has also been shown that poly(pyrrole) synthesized in the pores has a longer conjugation length (larger delocalization of the π-electrons) than ordinary PPy, facilitating the charge transport in the material and resulting in an increased conductivity.

REFERENCES

1 Burroughes, J. H., Jones, C. A. and Friend, R. H. *Nature* 1988, **335,** 137
2 Flytzanis, C. 'Nonlinear Behaviour of Molecules, Atoms and Ions', Elsevier, Amsterdam, 1979
3 Novák, P., Inganäs, O. and Bjorklund, R. *J. Electrochem. Soc.* 1987, **134,** 1341
4 Bartlett, P. N. and Birkin, P. R. *Synth. Met.* 1993, **61,** 15
5 Penner, R. M. and Martin, C. R. *J. Electrochem. Soc.* 1986, **133,** 2206
6 Cai, Z. and Martin, C. R. *J. Am. Chem. Soc.* 1989, **111,** 4138
7 Calahane, W. and Labes, M. M. *Chem. Mater.* 1989, **1,** 519
8 Martin, C. R. *Science* 1994, **266,** 1961
9 Cai, Z., Lei, J., Liang, W., Menon, V. and Martin, C. R. *Chem. Mater.* 1991, **3,** 960
10 Granström, M. and Inganäs, O. *Synth. Met.* 1993, **55–57,** 460
11 Pei, Q., Inganäs, O., Gustafsson, G., Granström, M., Andersson, M., Hjertberg, T., Wennerström, O., Österholm, J.-E., Laakso, J. and Järvinen, H. *Synth. Met.* 1993, **55–57,** 1221
12 Pei, Q., Zuccarello, G., Ahlskog, M. and Inganäs, O. *Polymer* 1994, **35,** 1347
13 Martin, C. R., Parthasarathy, R. and Menon, V. *Synth. Met.* 1993, **55–57,** 1165
14 Lundin, A., Lundberg, B., Saurerer, W., Nandery, P. and Naegele, D. *Synth. Met.* 1990, **39,** 233
15 Corish, J., Morton-Blake, D. A., Veluri, K. and Bénière, F. *J. Mol. Struct.* 1993, **283,** 121
16 Stewart, J. J. P. *J. Computer-Aided Mol. Design* 1990, **4,** 1
17 Dewar, M. J. S., Zoebisch, E. G., Healy, E. F. and Stewart, J. J. P. *J. Am. Chem. Soc.* 1985, **107,** 3902
18 Kiani, M. S., Bhat, N. V., Davis, F. J. and Mitchell, G. R. *Polymer* 1992, **33,** 4113
19 Kiani, M. S. and Mitchell, G. R. *Synth. Met.* 1992, **46,** 293
20 Druy, M. A. *Synth. Met.* 1986, **15,** 243
21 Kassim, A., Davis, F. J. and Mitchell, G. R. *Synth. Met.* 1994, **62,** 41
22 Liang, W. and Martin, C. R. *J. Am. Chem. Soc.* 1990, **112,** 9666
23 Mott, N. F. and Davis, E. A. 'Electronic Processes in Non-Crystalline Materials', Clarendon Press, Oxford, 1979
24 Maddison, D. and Tansley, T. L. *J. Appl. Phys.* 1992, **72,** 4677
25 Sheng, P., Abeles, B. and Arie, Y. *Phys. Rev. Lett.* 1973, **31,** 44
26 Sheng, P. *Phys. Rev. B* 1980, **21,** 2180
27 Sheng, P. and Klafter, J. *Phys. Rev. B* 1983, **27,** 2583
28 Wernet, W., Monkenbusch, M. and Wegner, G. *Makromol. Chem., Rapid Commun.* 1984, **5,** 157
29 Tian, B. and Zerbi, G. *J. Chem. Phys.* 1990, **92,** 3892
30 Liang, W., Lei, J. and Martin, C. R. *Synth. Met.* 1992, **52,** 227